SCA-9711

ANALYSIS OF CENTRIFUGE RELATIVE PERMEABILITY DATA

by
Douglas Ruth
University of Manitoba
Winnipeg, Manitoba, Canada

Abstract

This paper presents a simulation study of the displacement process that occurs during a multi-speed, centrifuge relative permeability experiment. Using Corey-type relative permeability and Bentsen-type capillary pressure curves, with parameters typical of water-wet rocks, synthetic production data sets are generated for a simulated drainage experiment. The sensitivities of the production data to small changes in the parameters of the curves are then tested. By examining the deviation between the resultant production data and the original data, different regions of the experiment are identified with sensitivities to different parameters. The production data is then "corrupted" by adding random errors. The resulting data sets are history-matched to determine the best curve parameters, that is, the parameters that result in the least-square-error between the "corrupted" data and a new simulation. As a final test, a production data set which includes the effect of ramp-up is generated, then history-matched assuming that speeds change in an instantaneous manner.

Introduction

The centrifuge technique for measuring relative permeability is a simple extension of the centrifuge technique for measuring capillary pressure — the fluid produced as a function of time for each rotational speed is analysed to determine the relative permeability curves. Data collection is therefore no more complicated than for the capillary pressure case except that the frequency of data capture is greatly increased, particularly just after the speed of rotation has been changed. For this reason, centrifuges that collect production data automatically have been developed. Descriptions of automated centrifuges may be found in O'Meara and Lease (1983), Munkvold and Torsæter (1990), King *et al* (1990), Hirasaki *et al* (1992b), Nikakhtar *et al* (1994), and Kantzas *et al* (1995). Other centrifuge relative permeability studies include van Spronsen (1982), O'Meara and Crump (1985), Torsæter and Munkvold (1987), Firoozabadi and Aziz (1991), Hirasaki *et al* (1992a), Chardaire *et al* (1992), Nordtvedt *et al* (1993), and Fleury *et al* (1994).

Two techniques are used to analyse production data to obtain relative permeability curves: the Hagoort (1980) method and numerical simulation. The Hagoort method is based on three assumptions: that the effects of capillary pressure are negligible except near the equilibrium point (a correction procedure is available); that the acceleration is uniform along the sample; and that the mobility of the non-wetting component is infinite. These assumptions lead to a particularly simple formulation for the determination of the relative permeability curve of the wetting component, particularly if a Corey equation is used to model this curve. In the present paper, interest will focus on the more general case of finite capillary pressure, non-uniform acceleration, and finite mobility of the non-wetting component. Numerical simulation allows for full consideration of the general case.

Formulation of the Simulation Model

It will be assumed that a wetting fluid is being displaced by a less dense non-wetting fluid. The analysis of the transient flow that results from an increment in the rotation

speed of the centrifuge is based on the following set of equations (Kantzas *et al* 1995):

$$q_{nw} = -\frac{k\, k_{rnw}\, A}{\mu_{nw}} \frac{d}{dr}\left(P_{nw} - \frac{\rho_{nw}\, \omega^2\, r^2}{2}\right) , \tag{1}$$

$$q_w = -\frac{k\, k_{rw}\, A}{\mu_w} \frac{d}{dr}\left(P_w - \frac{\rho_w\, \omega^2\, r^2}{2}\right) , \tag{2}$$

and

$$P_c = P_{nw} - P_w \, . \tag{3}$$

In these equations, the q's are the flow rates, k is the absolute permeability, the k_r's are the relative permeabilities, the μ's are the viscosities, A is the cross-sectional area, the P's are the pressures, the ρ's are the densities, ω is the rotational speed, r is the radius from the center of rotation, P_c is the capillary pressure, and the subscripts w and nw denote the wetting and non-wetting components respectively. These equations may be solved simultaneously to yield an equation for the flow rate of the wetting component:

$$q_w = \frac{k_{rw}\, \mu_{nw}}{k_{rw}\, \mu_{nw} + k_{rnw}\, \mu_w} \left[q_t + \frac{k_{rnw}\, k\, A}{\mu_{nw}} \left(\frac{dP_c}{dr} + \frac{d}{dr}\left(\Delta\rho \frac{\omega^2\, r^2}{2}\right)\right)\right] . \tag{4}$$

where q_t is the total flow rate (the sum of q_w and q_{nw}) and $\Delta\rho = \rho_w - \rho_n w$.

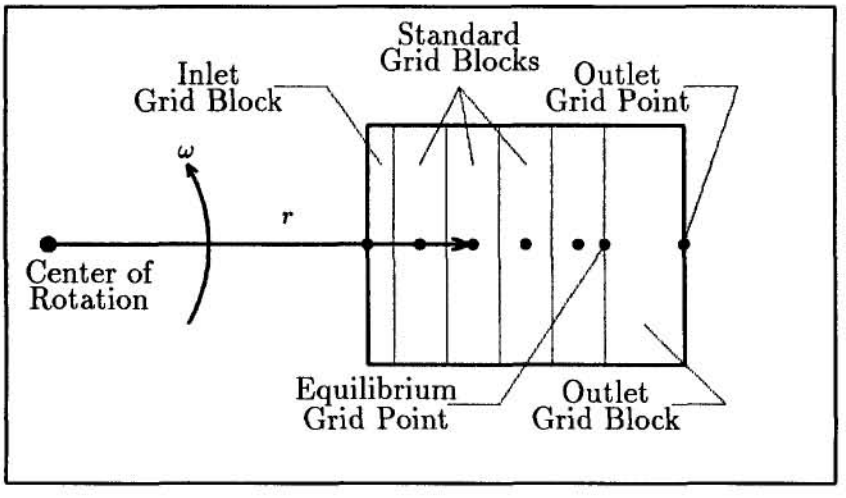

Figure 1 The Finite Difference Grid System

At equilibrium, after the flow has ceased at any rotational speed, the capillary pressure as a function of radius from the center of rotation is given by

$$P_c = \frac{\Delta\rho\, \omega^2}{2} \left(r_o^2 - r^2\right) , \tag{5}$$

where r_o is the distance to the outlet face of the sample. Figure 1 shows the grid system that is used in the present paper. In this system, the equilibrium grid point

is the location determined by the threshold capillary pressure, P_{ct}. Setting $P_c = P_{ct}$ and solving Equation 5 for r (denoted now as r_t) results in the expression

$$r_t = \sqrt{r_o^2 - \frac{2\,P_{ct}}{\Delta\rho\,\omega^2}}\,. \tag{6}$$

The equilibrium grid point is located in a zero width grid block; there is no flow of the non-wetting component in this grid block or in the outlet grid block. The inlet grid block is made half the size of other grid blocks in order to allow the location of a grid point on the inlet surface. The outlet grid point will have the pressures

$$P_w = P_{nw} = P_c = 0\,. \tag{7}$$

When the speed of rotation is changed, the grid system is augmented with extra grid blocks, the last of which has an outlet face location dictated by the equilibrium location of the threshold capillary pressure and the new speed. Because the sample is surrounded by the non-wetting component, the pressure at the inlet grid point may be determined by analysing the pressure in the non-wetting component outside of the sample. Such an analysis results in the equation

$$P_{nw} = -\frac{\rho_{nw}\,\omega^2}{2}\,(r_o^2 - r_i^2)\,, \tag{8}$$

where r_i is the radius of the inlet grid point.

The simplest procedure for simulating incompressible, two component flow is based on knowing the total flow rate and the saturations at all grid points at the start of a time step, then assuming that the total flow rate is known, an explicit simulation scheme may be implemented. Using the total flow rate and the saturations, the flow rates of the wetting component at each location are calculated using Equation 4. Once known, these flow rates are used to calculate changes in saturations. The procedure is then repeated. In this manner, the saturations, production, and pressure field may be calculated at any desired time.

However, the total flow is not known *a priori* in the case of transient flow in a centrifuge experiment, but the pressure of the non-wetting component at the inlet face is a known quantity (Equation 8) and can be used to determine the total flow rate. An expression for the pressure gradient may be found by summing Equations 1 and 2, making use of Equation 3, and solving for the gradient:

$$\begin{aligned}\frac{dP_w}{dr} = &-\frac{\mu_{nw}\,\mu_{nw}}{\mu_w\,k_{rnw} + \mu_{nw}\,k_{rw}} \\ &\left[\frac{q_t}{k\,A} + \frac{k_{rnw}}{\mu_{nw}}\frac{dP_c}{dr} - \frac{k_{rnw}}{\mu_{nw}}\frac{d}{dr}\left(\frac{\rho_{nw}\,\omega^2\,r^2}{2}\right) - \frac{k_{rw}}{\mu_w}\frac{d}{dr}\left(\frac{\rho_w\,\omega^2\,r^2}{2}\right)\right].\end{aligned} \tag{9}$$

At any instant, the total flow, must be constant along the sample. Equation 9 may therefore be integrated numerically. The left hand side yields the pressure at the inlet in the wetting component, which may be converted to the pressure in the non-wetting component using the capillary pressure equation. The pressure in the non-wetting component is calculated using Equation 8; therefore the value of q_t may be calculated. Once q_t is known, the methodology outlined above may be used to simulate the flow.

The accuracy of any simulation is controlled by the number of grid blocks used and the size of the time step. In the numerical model used to generate the data for the present paper, the number of grid blocks varies with speed. Control of grid block size is achieved by specifying the number of grid blocks for the initial speed. When grid blocks are added at different speeds, the rules applied are as follows:

1. If the added grid block is less than 0.3 of the width of the standard grid block at the first speed, no grid blocks are added; instead, the last full grid block is expanded.
2. If the added region is greater than 1.3 of the width of the standard grid block at the first speed, a sufficient number of standard width grid blocks are added, plus one non-standard width grid block to accomodate the new equilibrium position.

Time step control is achieved by specifying the maximum allowable saturation change in a grid block.

The present study considers relative permeability curves specified by Corey equations of the form

$$k_{wr} = k_{wre}\left(\frac{S_w - S_{wr}}{1 - S_{wr} - S_{nwr}}\right)^{n_w} \tag{10}$$

and

$$k_{nwr} = k_{nwre}\left(\frac{S_{nw} - S_{nwr}}{1 - S_{wr} - S_{nwr}}\right)^{n_{nw}}, \tag{11}$$

where thw S's are the saturations, and the subscripts denote the following: r (on k), relative; e, endpoint; and r (on S), residual. The capillary pressure is specified by a Bentsen curve

$$P_c = P_{ct}\left[1 - Be\,ln\left(\frac{S_w - S_{wr}}{1 - S_{wr} - S_{nwr}}\right)\right], \tag{12}$$

where P_{ct} is the threshold pressure, and Be is the Bentsen number (see Ruth and Wong 1990). Capillary pressure curves for which P_c changes significantly as saturation changes are characterized by high Bentsen numbers while capillary pressure curves that are relatively flat are characterized by low Bentsen numbers.

Test Parameter Specification

For the present study, a system with the parameters listed in Table 1 were assumed. Table 2 shows the schedule for the experiment.

In order to identify appropriate values for the initial number of grid blocks (N) and the maximum saturation change in a grid block (ΔS), a sensitivity study was performed. For $\Delta S = 0.001$, a production history was generated for $N = 10$. Production histories were then generated for a range of values of N and the root-mean-square difference (ϵ) in production between each data set and the $N = 10$ data set was calculated. The results are presented in Figure 2. A detailed examination of the production histories showed that the differences observed for lower values of N occur primarily in the lower speed ranges. As N increases, larger differences occur at higher speeds. The reason for this behaviour is that the saturation profile is confined to a smaller region at higher speeds. The number of grid blocks in this region is small when N is small. As N increases, the ability of the simulation to accurately predict the behaviour of the fluids at higher speeds improves and larger differences result. Based on the results of this study, a value of $N = 40$ was choosen for further studies.

Using a value of $N = 40$, a study of the sensitivity of the simulations to the value of ΔS was performed. The results are given in Figure 3. This figure shows that

Variable	Value	Units
Porosity	0.25	-
Permeability	100.0	md
Length	5.08	cm
Diameter	3.18	cm
r_o	9.38	cm
ρ_w	1000.0	kg/m^3
ρ_{nw}	850.0	kg/m^3
μ_w	1.00	cp
μ_{nw}	1.00	cp
S_{wr}	0.20	-
S_{nwr}	0.00	-
k_{wre}	0.25	-
k_{nwre}	1.00	-
n_w	2.00	-
n_{nw}	2.00	-
Be	8.00	-
P_{ct}	1.00	kPa

Table 1 Sample and Fluid Properties

Time (min)	Speed (rpm)
0.0	600
480.0	1000
960.0	2000
1440.0	4000
1920.0	8000
2400.0	end

Table 2 Schedule

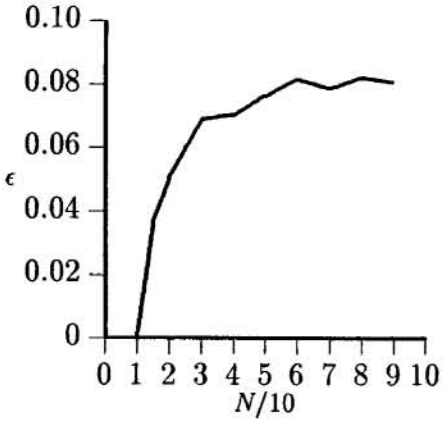

Figure 2 The Grid Block Study

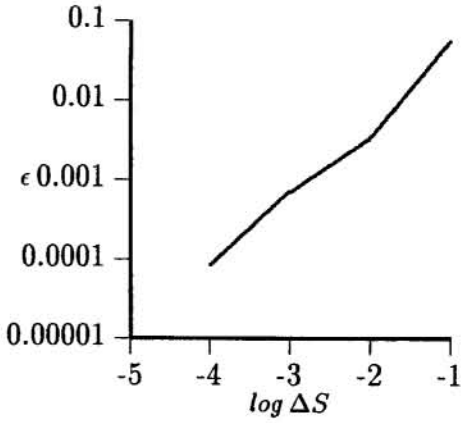

Figure 3 The Time Step Study

errors due to ΔS are small relative to errors due to N, provided $\Delta S < 0.01$. A value of $\Delta S = 0.001$ was choosen for further studies.

Error Limits for Fitting Parameters

Analysis of experimental data to determine relative permeability and capillary pressure curves involves a history-matching process using fitting parameters. In the context of the present study, these fitting parameters are the saturation exponents for the relative permeability curves and the values of P_{ct} and Be for the capillary pressure curve. Typically the values of k_{re} and S_r are not used (they are determined independently, although there is no fundamental reason why they could not be included in the history-matching procedure). A sensitivity study was conducted to determine how accurately the values of these fitting parameters can be determined for various scenarios. The procedure for this study was to generate a production history for a given set of parameters, then to vary the value of each fitting parameter and calculate the root-mean-square difference in production. The change in the fitting parameter

required to cause a root-mean-square difference equal to the assumed experimental error (based on an experimental error of $0.06\,cm^3$) was then calculated. The results are summarized in Table 3. The properties studied were the saturation exponents (shape of the relative permeability curves), Be (the shape of the capillary pressure curve), and the viscosity (mobility ratio). The results of the study show the following:

1. The saturation exponent for the wetting component can generally be found with good accuracy regardless of the operating parameters. The sensitivity is relatively constant for all of the variables studied.
2. The accuracy to which the saturation exponent of the non-wetting component may be found is generally poor except for the case of a high viscosity non-wetting component.
3. Sensitivity to both capillary pressure parameters is generally good.

New Value of Variable	Sensitivities (Error Bars ±)			
	n_{nw}	n_w	P_{ct}	Be
Base Case	0.29	0.15	0.10	0.25
$\mu_{nw} = 10.0\,cp$	0.15	0.18	0.11	0.23
$\mu_{nw} = 0.1\,cp$	0.71	0.14	0.10	0.25
$\mu_{nw} = 0.01\,cp$	2.59	0.14	0.10	0.26
$n_{nw} = 4.0$	0.19	0.14	0.11	0.21
$n_{nw} = 8.0$	0.28	0.15	0.15	0.17
$n_w = 4.0$	0.31	0.14	0.11	0.34
$n_w = 8.0$	0.32	0.20	0.12	0.44
$Be = 2.0$	0.38	0.15	0.04	0.07
$Be = 1.0$	0.45	0.12	0.03	0.04
$Be = 0.5$	0.62	0.11	0.02	0.03

Table 3 Results for the Sensitivity Study

Details of the Displacement

The various fitting parameters have different influences during different parts of the experiment. Figure 4 shows the absolute errors for the base case caused by varying the values of n_{nw}, n_w, and Be by 5%. The first thing to note is that an error in the capillary curve (Be) influences the error throughout the entire experiment. This is because the capillary pressure influences the maximum production at each speed; hence errors in the capillary pressure curve produce differences in the production values that persist from one speed to the next. One way to overcome the dominance of capillary pressure is to fit incremental production, not cumulative production. However, this is problematic for centrifuge data because the errors of observation are often of the same magnitude as the differences in production (unless the data is heavily smoothed or a lot of the data is discarded). The best solution to this problem is to not use capillary pressure parameters in the fitting procedure. Capillary pressure can be determined separately using only the production values at the end of each speed range (see Ruth and Chen (1995) for a summary). Values obtained in this manner should not be varied when obtaining a fit for the relative permeability. Further examination of Figure 4 shows that the influence of n_{nw} is confined to the first speed range, the early part of the second speed range, and the very early part of the third speed range. The influence of n_w is confined to early parts of each speed ranges except the first and second. Therefore, in this particular case, the regions of influence for the two exponents is almost completely decoupled.

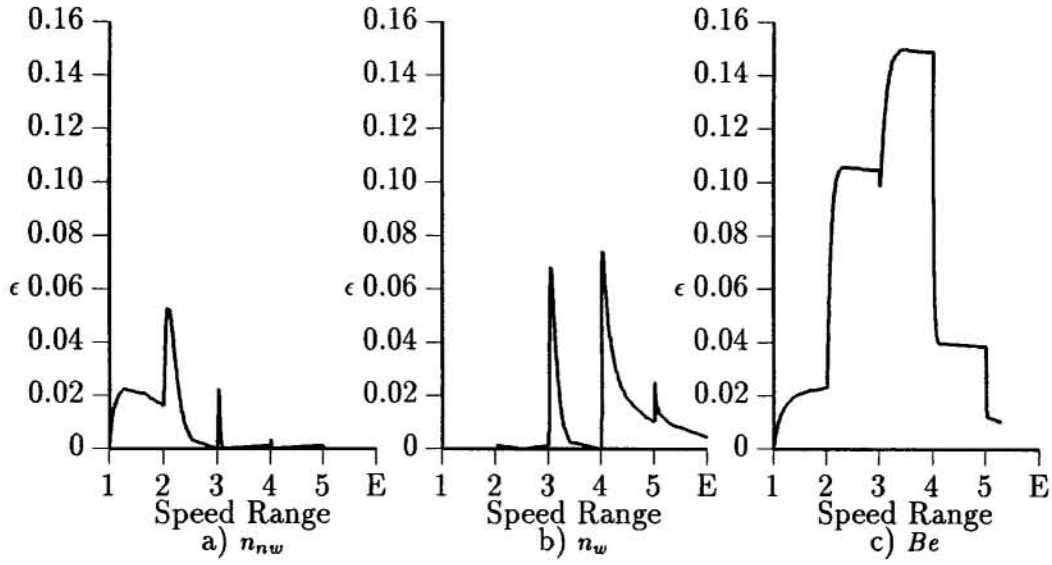

Figure 4 Absolute Differences Caused by Varying Parameters (Base Case)

Figure 5 shows the absolute errors calculated for the case where the viscosity is reduced to 0.1 *cp* with all other properties of the base case held constant. This change modifies the behaviour of the error as compared to that shown in Figure 4. The deviations caused by changes in n_{nw} have been reduced, thereby decreasing the ability to obtain accuate values for this parameter. The influences of the other two parameters remain strong. Figure 6 shows results for a reduced capillary pressure case. Again the relative importance of the various parameters has changed.

Although no general conclusions can be drawn based on these three examples, the importance of investigating the influence of the various parameters is clear. In particular, the experimental speed ranges must be choosen carefully if estimates for the exponent for the non-wetting component are to be obtained. Strictly speaking, the present results apply only to Corey equation relative permeabilities. However, these equations were used only as a convenience; the complex dependence of the curves on the operating parameters will almost certainly be observed regardless of the technique used to model the curves. Furthermore, the present model neglects radial and Earth-gravity effects. These effects will undoubtably influence the results, however, they are generally of secondary importance and therefore should not have a major influence on the final conclusions.

The above observations suggest the following fitting strategies:

1. Determine the capillary pressure parameters separately and do not use them in the history matching process.
2. Pre-treat the data to select for early times in a speed range.
3. Accept the fact that the wetting-component relative permeability will be more accurately obtained than will the non-wetting-component relative permeability.

Examples

To further evaluate some of the problems encountered in history matching data, a

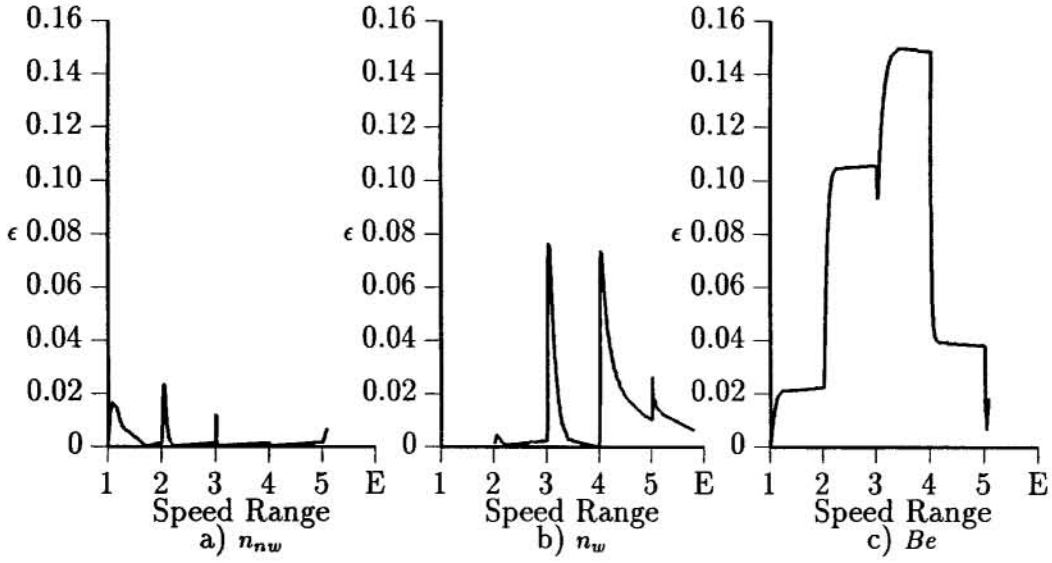

Figure 5 Absolute Differences Caused by Varying Parameters
($\mu_{nw} = 0.1\,cp$)

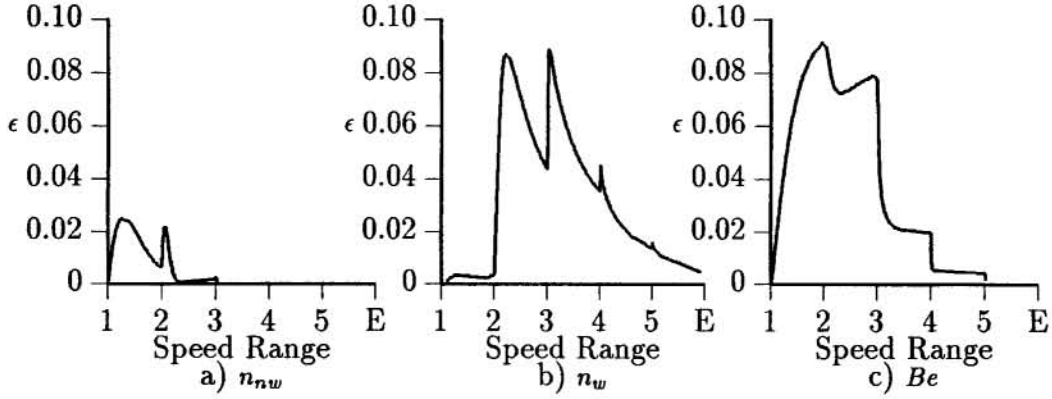

Figure 6 Absolute Differences Caused by Varying Parameters
($Be = 1.0$)

model data set was generated using the basic case parameters and $N = 90$. This data set was then history matched using $N = 10$, $N = 20$, and $N = 40$. These matches were achieved by varying n_w and n_{nw} until the root-mean-squared difference between the $N = 90$ data set and the new data set was minimized. Next the data set was "corrupted" by adding random errors to the production values. Usually, when corrupting data, errors with a normal distribution are added. However, in automated centrifuges, the measurement of production is usually made using a linear array of optical sensors. This is a digital device and errors have both a resolution component and a random component to them. To recognize this fact, errors with a uniform distribution having a standard deviation equal to the assumed error ($0.06\ cm^3$) were added. This procedure results in larger errors than would be realized using a normal distribution.

As a final test, a data set that includes the influence of speed "ramp-up" was generated. The acceleration for the ramp-up was assumed to be $1000\,rpm/m$. (This value

represents an extreme case. Hirasaki *et al* (1992a) quote a much higher acceleration of $5000\,rpm/m$.) This data set was then history matched assuming that no ramp-up occured, that is, that the speed changed instantaneously at each increment.

The results for these further tests are shown in Table 4. The effect of the number of grid blocks is seen to be small, although more grid blocks clearly lead to better results. For $N = 10$, the estimate of n_w is outside of the error bars determined in Table 3 and the value of ϵ is still high. This value drops significantly for $N = 20$ and the value of n_w lies within the error bars. Similarly, provided that the errors are random (the "corrupted" case), they have little effect on the final values of the exponents; however, as expected, the value of ϵ is large, being approximately equal to the standard deviation of the random experimental error imposed on the data. The ramp-up process introduces systematic errors; if not properly accounted for, these errors lead to a significant difference in the value of n_w. The smaller effect on n_{nw} is due to the generally smaller sensitivity of this parameter.

Test Type	n_{nw}	n_w	ϵ
Base Case: $N = 90$	2.000	2.000	0.0000
Clean Data: $N = 10$	2.076	1.867	0.0587
Clean Data: $N = 20$	2.058	1.928	0.0235
Clean Data: $N = 40$	2.019	1.975	0.0074
Corrupted Data: $N = 10$	2.076	1.868	0.0825
Corrupted Data: $N = 20$	2.051	1.931	0.0631
Corrupted Data: $N = 40$	2.061	1.931	0.0631
Ramp-Up Data: $N = 40$	2.023	2.195	0.1255

Table 4 Results of Various Problem Data Sets

Conclusions

The conclusions, in the form of recommended operating and analysis procedures, based on the present work are as follows:

1. The capillary pressure should be found by direct calculation and should not be part of the history-matching process.
2. If accurate non-wetting-component relative permeability curves are required, care must be taken to select speed ranges that result in capillary pressures very near the threshold value. This results is displacements that are controlled by the relative permeability of the non-wetting component, not the wetting component.
3 The wetting-component curve is most sensitive to data obtained just after a speed change. Data sets should be pre-treated to select a prepondenance of such data.
4. Ramp-up data should be properly accounted for, particularly if the ramp-up is conducted slowly.

References

Chardaire-Rivière,C., P.Forbes, J.F.Zhang, G.Chavent and R.Lenormand, "Improving the Centrifuge Technique by Measuring Local Saturations," *SPE Annual Technical Conference and Exhibition,* (67th), Washington, D.C., October 4-7, [SPE 24882], 1992.

Firoozabadi,A. and K.Aziz, "Relative Permeability from Centrifuge Data," *JCPT,* Vol.30, No.5, pp.33-42, 1991.

Fleury,M., R.Lenormand and F.Deflandre, "Interpretation of Centrifuge Data using Local Saturation," *SCA Annual Technical Conference,* (8th), Stavanger, Norway, September 12-14, [SCA 9428], 1994.

Hagoort,J., "Oil Recovery by Gravity Drainage," *SPEJ,* Vol.20, No.6, (June), [SPE 7424], pp.139-150, 1980.

Hirasaki,G.J., J.A.Rohan and J.W.Dudley, "Interpretation of Oil/Water Relative Permeabilities from Centrifuge Experiments," *SPE Annual Technical Conference and Exhibition,* (67th), Washington, D.C., October 4-7, [SPE 24879], 1992a.

Hirasaki,G.J., J.A.Rohan and J.W.Dudley, "Modification of Centrifuge and Software for Determination of Relative Permeability Curves," *SPE Unsolicited Paper,* [SPE 25290], 1992b.

Kantzas,A., B.Nikakhtar, D.Ruth and M.Pow, "Two Phase Relative Permeabilities Using the Ultracentrifuge," *JCPT,* Vol.34, No.7, (september), pp.56-63, 1995.

King,M.J., K.R.Narayanan and A.J.Falzone, "Advances in Centrifuge Methodology for Core Analysis," *SCA Annual Technical Conference,* (4th), Dallas, Texas, August 14-16, [SCA 9011], 1990.

Munkvold,F. and O.Torsaeter, "Relative Permeability from Centrifuge and Unsteady State Experiments," *SPE Latin American Petroleum Engineering Conference,* Rio de Janerio, Brazil, October 14-19, [SPE 21103], 1990.

Nikakhtar,B., A.Kantzas, P.de Wit, M.Pow and A.George, "On the Characterization of Rock/Fluid and Fluid/Fluid Interactions in Carbonate Rocks Using the Ultracentrifuge," *JCPT,* Vol.35, No.1, (January), pp.47-56, 1996.

Nikakhtar,B., A.Kantzas, F.Wong and M.Pow, "Some Observations on the Capillary Pressure Hysteresis using the Ultracentrifuge," *SCA Annual Technical Conference,* (8th), Stavanger, Norway, September 12-14, [SCA 9423], 1994.

Nordtvedt,J.E., G.Mejia, P.Yang and A.T.Watson, "Estimation of Capillary Pressure and Relative Permeability Functions from Centrifuge Experiments," *SPERE,* Vol.8, No.4, (November), [SPE 20805], pp.292-298, 1993.

O'Meara,D.J.Jr. and J.G.Crump, "Measuring Capillary Pressure and Relative Permeability in a Single Centrifuge Experiment," *SPE Annual Technical Conference and Exhibition,* (60th), Las Vegas, Nevada, September 22-25, [SPE 14419], 1985.

O'Meara,D.J.Jr. and W.O.Lease, "Multiphase Relative Permeability Measurements Using an Automated Centrifuge," *SPE Annual Technical Conference and Exhibition,* (58th), San Francisco, California, October 5-8, [SPE 12128], 1983.

Ruth,D.W. and Z.A.Chen, "Measurement and Interpretation of Centrifuge Capillary Pressure Curves — The SCA Survey Data," *The Log Analyst,* Vol.36, No.5, (September-October), pp.21-33, 1995.

Ruth,D. and S.Wong, "Centrifuge Capillary Pressure Curves," *JCPT,* Vol.29, No.3, (May-June), pp.67-72, 1990.

Torsæter,O. and F.R.Munkvold, "Automated Centrifuge for Measurement of Capillary Pressure and Relative Permeability," *European Symposium on Enhanced Oil Recovery,* (4th), Hamburg, Germany, October, pp.999-1006, 1987.

van Spronsen,E., "Three-Phase Relative Permeability Measurements using the Centrifuge Method," *SPE/DOE Symposium on Enhanced Oil Recovery,* (3rd), Tulsa, Oklahoma, April 4-7, [SPE/DOE 10688], 1982.